THE JOURNAL OF PHYSICAL CHEMISTRY B

Article

pubs.acs.org/JPCB

pH-Replica Exchange Molecular Dynamics in Proteins Using a Discrete Protonation Method

Danial Sabri Dashti,[†] Yilin Meng,[‡] and Adrian E. Roitberg*[,§]

[†]Department of Physics and Quantum Theory Project and [§]Department of Chemistry and Quantum Theory Project, University of Florida, Gainesville, Florida 32611-8435, United States

[‡]Department of Biochemistry and Molecular Biology, University of Chicago, Chicago, Illinois 60637, United States

ABSTRACT: Protonation equilibria in biological molecules modulates structure, dynamics, and function. A pH-replica exchange molecular dynamics (pH-REMD) method is described here to improve the coupling between conformational and protonation sampling. Under a Hamiltonian replica exchange setup, conformations are swapped between two neighboring replicas, which themselves are at different pHs. The method has been validated on a series of biological systems. We applied pH-REMD to a series of model compounds, to an terminally charged ADFDA pentapeptide, and to a heptapeptide derived from the ovomucoid third domain (OMTKY3). In all of those systems, the predicted pK_a by pH-REMD is very close to the experimental value and almost identical to the ones obtained by constant pH molecular dynamics (CpH MD). The method presented here, pH-REMD, has the advantage of faster convergence properties due to enhanced sampling of both conformation and protonation spaces.

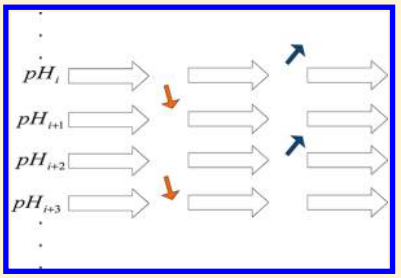

INTRODUCTION

Solution pH plays a very important role in protein function, dynamics, and structure. Many important biological phenomena function only at a certain range of pH's, including protein folding/misfolding,[1−3] enzyme catalysis,[4−6] and ligand−substrate docking.[7,8] In those cases, a pH change leads to a change in the ratio of protonation states of different titratable residues, which is usually coupled to a change in the conformation and dynamics of the protein itself.

The pK_a of a titratable residue is the pH value at which the ratio of deprotonated to protonated concentrations of that residue is equal to 1.[9−12] The pK_a of an ionizable residue in a protein is highly dependent on its electrostatic environment, which is coupled to the protonation states of other titratable groups and the conformation state of the protein. Most current simulations of pH-dependent properties do not, in fact, change protonation states during molecular dynamics but rather pick a certain set of protonation states using educated guesses or guided by simplified algorithms and then keep it constant for the remainder of the simulation. These constant-protonation MD methods suffer from two big disadvantages.[13] First, at a pH near the pK_a of any of the titratable residues, any possible choice of constant protonation would clearly be wrong. Second, the choice of protonation state is coupled for neighboring residues, which itself couples to the conformational space of the system.

Like concentration and temperature, the solution pH is a very useful external and controllable variable in experimental methods. Hence, the importance of constant pH MD (CpH MD) has been recognized. In the last 2 decades, many constant pH MD methods have been developed.[14,15] The goal of CpH MD is to describe correctly the protonation equilibrium coupled by conformation equilibrium at a certain pH. The majority of CpH MD methods can be divided into continuous[14−22] and discrete[13,23−32] protonation state methods.

Continuous protonation methods use a continuous protonation parameter to perturb the ionizable residue between protonated and deprotonated states. In 1994, Mertz and Pettitt[21] developed a grand canonical method for simulating a simple chemical reaction. They applied the method for exchanging a proton between water molecules and an ionizable side chain. In 1997, Baptista et al.[14] introduced a continuous constant pH method in implicit solvent based on a mean-field approximation. In 2001, Börjesson et al.[15] used a weakly coupled proton bath to continuously adjust the protonation fraction of each titratable group toward equilibrium. More recently, the Brooks group has developed the continuous protonation state method further.[16−20,33] In the case of highly coupled titration groups, where cooperativity effects are non-negligible, this model leads to inappropriate estimation of physical variables. To alleviate this problem, Lee et al.[33] added a biasing potential, centered at $\lambda = 0.5$, to help drive the protonation coordinate value to fully protonated/deprotonated states and away from the mid-λ unphysical states.

In contrast to the continuous protonation state methods, the discrete protonation models define the protonation state of the ionizable group as either zero or one during the simulation, corresponding to protonated and deprotonated states only. These models use a hybrid MD−MC scheme; the MD is used

Received: April 9, 2012
Revised: June 4, 2012
Published: June 13, 2012

   dx.doi.org/10.1021/jp303385x | J. Phys. Chem. B 2012, 116, 8805−8811

to sample conformational space for a number of steps, after which a Metropolis MC[34] attempt will be done for changing the protonation state/states. A new set of MD steps is then done with the protonation state chosen by the MC step, and the process is repeated. Many versions of the constant pH/discrete protonation MD method have been developed.[13,24−29,31,32,35,36] The Baptista group[23−26,36] used explicit solvent for the propagation of coordinates and the Poisson−Boltzmann (PB) method for calculating the energy in the MC section of the algorithm; Walczak et al.[32] employed Langevin dynamics for MD and the PB method for both of the MC and MD steps. Bürgi et al.[27] applied the thermodynamic integration method (TI) to calculate the transition energy between the protonated and deprotonated species in explicit solvent MD. The drawback for this approach is the large computational cost of TI calculation, which limits the amount of sampling in protonation space. In 2004, Mongan et al. developed a discrete protonation MD method by using the generalized Born (GB) implicit solvent method for both the MD (structure) and MC (protonation state) sampling sections.[13] A more detailed explanation of the method can be found in the Theoretical Method and Simulation Details section. This method is implemented in the AMBER molecular dynamics package.[37]

It has become clear in recent years that accurate modeling of protonation space also requires enhanced sampling of conformational space.[38−40] Accurate sampling of the conformational space of proteins remains a challenging area. Many theoretical methods have been proposed to overcome the free-energy barriers in conformational space. Among those, generalized ensemble methods[41−43] such as replica exchange MD (REMD),[44] simulated tempering[45] (ST), multicanonical ensemble,[46,47] metadynamics,[48] and orthogonal space random walk[49] (OSRW) are well-established. In some of those methods, in addition to conformational space (i.e., regular MD), the system is made to perform a random walk in energy or temperature space, reducing conformational trapping.

To account for the coupling of protonation and conformational sampling, Khandogin et al.[50] have recently combined the continuous protonation constant pH MD with the REMD method (REX-CPHMD). They applied it to the problems of pK_a prediction protein folding and pH-dependent conformation, among others.[50,51] Recently, Meng and Roitberg[52] utilized a hybrid method by combining the temperature REMD (T-REMD) and discrete protonation constant pH MD.

In the present article, we introduce a method for pH-exchange MD by combining the discrete protonation constant pH MD (proposed by Mongan et al.[13]) and Hamiltonian REMD (H-REMD).[53]

We tested our method by applying it to five model dipeptides, to an uncapped pentapeptide with sequence $^{+}H_3N$-Ala-Asp-Phe-Asp-Ala-COO^{-} (ADFDA), and to an heptapeptide derived from the ovomucoid third domain OMTKY3 protein. Because the two ends of ADFDA are not capped, its two Asp residues have slightly different electrostatic environments, and their pK_as deviate in different directions from the pK_a of unperturbed Asp. We will show that the pH-REMD improves the sampling efficiency in both protonation and conformation spaces.

In the rest of this paper, constant pH MD (CpH) refers to Mongan's CpH MD approach, unless mentioned otherwise.

THEORETICAL METHOD AND SIMULATION DETAILS

CpH MD and pH-REMD. The goal of CpH MD is to sample the equilibrium between protonated and deprotonated state of titratable sites at a given pH. The free-energy difference between protonated and deprotonated states determines the ratio of their concentrations. This free-energy difference cannot be calculated by molecular mechanics (MM) because the change in protonation state involves a bond breaking/forming phenomena, which requires a series of highly accurate quantum calculations. To address this issue, a method,[13,35,54] which uses a precalculated pK_a of reference compounds, has been developed. Reference/model compounds, in AMBER terminology, are represented by a capped dipeptide for each titratable residue (i.e., ACE-titratable residue NME). The free energy for the protonation change to be used in the MC criteria is described by Mongan[54] et al. as

$$\Delta G_{\text{protein}} = \Delta G_{\text{protein,MM}} + k_B T(\text{pH} - \text{p}K_{\text{a,ref}}) \ln 10 - \Delta G_{\text{ref,MM}} \quad (1)$$

where T is the temperature and k_B is the Boltzmann constant. $\Delta G_{\text{protein,MM}}$ is the MM part of free energy of the titratable site in the protein, and $\Delta G_{\text{ref,MM}}$ is the precomputed deprotonation free energy for the reference compound, described above. Using eq 1, there is no need to calculate the QM contribution to the free energy in the protein. This method is implemented in the AMBER MD suite,[37] using the GB implicit solvent model. Every few MD steps, a Metropolis MC attempt will be done[34] to change the protonation state of the titratable residue, and $\Delta G_{\text{protein}}$ will be used to make a decision about accepting or rejecting the proposed MC move. In other word, the MC moves will sample protonation space, and the MD steps will sample configuration space. During the MD steps, the protonation state is kept constant.

Titration Curve. The pK_a of a titratable residue is related to pH environment through the Henderson−Hasselbalch (HH) equation

$$\text{p}K_a = \text{pH} - n \log\left(\frac{[A^-]}{[HA]}\right) \quad (2)$$

with $[A^-]$ and $[HA]$ being the deprotonated and protonated concentrations, respectively; n is the Hill coefficient, which should approach 1 for noninteracting ionizable residues, deviating from 1 in the case of interacting titratable residues because of cooperativity.[55]

Because of the ergodicity assumption underlying in MD, the ratio of the time that the titratable residue spends in deprotonated states to the time that it spends in protonated state can be considered as a ratio of the concentration of the deprotonated state to that of the protonated state.

On other hand, pH-REMD is a combination of CpH and H-REMD.[53] In contrast to temperature replica exchange,[44] in which each replica runs at a different temperature, in H-REMD, each replica runs in a distinct Hamiltonian but at the same temperature. In pH-REMD, each replica runs a constant pH MD at a unique pH, and periodically, an exchange of conformation between two adjacent replicas is attempted (see Appendix A for more information about the pH-REMD method).

We note that a recent publication[49] presented a pH-replica exchange method using a different exchange criterion that does

dx.doi.org/10.1021/jp303385x | J. Phys. Chem. B 2012, 116, 8805−8811

Table 1. pK_as of the Reference Compounds Computed by Different Methods

	ASP	GLU	HIS	TYR	LYS
experimental value	4.0	4.4	6.3	9.6	10.5
CpH MD	3.9 ± 0.1	4.4 ± 0.1	6.3 ± 0.1	9.6 ± 0.03	10.4 ± 0.03
pH-REMD	3.9 ± 0.1	4.4 ± 0.1	6.4 ± 0.1	9.7 ± 0.02	10.4 ± 0.04

not require recomputing energies for different replicas. In the future, we will compare the two formulations.

Simulation Details. In order to validate and test method presented here, we choose and ran simulations on three categories of systems. First, we studied the capped reference compounds (described in the methods sections), consisting the ACE-titratable residue NME.

Simulation times were 3 ns for both CpH MD and pH-REMD (for each replica) methods. We used eight pH replicas for all of the model compounds in pH-REMD.

We also tested our simulation method on a terminally charged pentapeptide model, ADFDA. Because the two ends of ADFDA are oppositely charged, the two Asp amino acids experience different electrostatic environments and have different pK_as. The simulation times of ADFDA were 90 ns for CpH and 10 ns for each replica in pH-REMD. Eight replicas, at pH = 2.5−6.0 with an increment of 0.5, were used in the pH-REMD method.

The third system was a heptapeptide derived from OMTKY3 (ACE-Ser-Asp-Asn-Lys-Thr-Tyr-Gly-NME). We simulated 100 ns for CpH and 10 ns for pH-REMD. Twelve replicas, at pH = 2−13 with increment of 1 pH unit, were used in pH-REMD method.

All calculations in this paper were done using the AMBER 10 molecular simulation suite. The AMBER ff99SB force field[56] and OBC GB implicit solvent[57] (igb = 2) were used in all simulations. The Shake algorithm[58] was applied to constrain the bonds between heavy and hydrogen atoms, which allowed the use of 2 fs MD steps. The cutoff of 30 Å for nonbonded interactions was chosen in all calculations.

In all pH-REMD simulations, except the heptapeptide derived from OMTKY3, replicas attempted a pH exchange every 1000 MD steps. In the case of the heptapeptide, replicas attempted a pH exchange every 500 MD step to accelerate sampling.[59] The exchange acceptance ratios between replicas for all systems were between 0.2 and 1.0. For calculating the error bars and the uncertainty of pK_as, every 4000 MC steps (in protonation space), the deprotonation fraction was calculated.

RESULTS AND DISCUSSION

1. Titratable Model Compounds. When we apply pH-REMD to the model compounds that were initially used to parametrize the method, it is not surprising to find that it produces the correct pK_as. It is, however, an important calculation to perform to check the method and to gauge its efficiency versus constant pH runs. The results are shown in Table 1 where all pK_a values have been calculated by a fit to the linearized version of the HH equation.

In Figure 1, the Hill plots for capped lysine has been plotted for both pH-REMD and CpH MD methods; it shows agreement among them over a large pH range.

2. ADFDA Model Compound. We now apply the method to the model peptide, ADFDA, that has charged ends. This system has an intrinsic but subtle asymmetry in the electrostatic environment for the two Asp ionizable side chains. Asp2 is close to the NH_3^+, which makes its pK_a be shifted slightly below

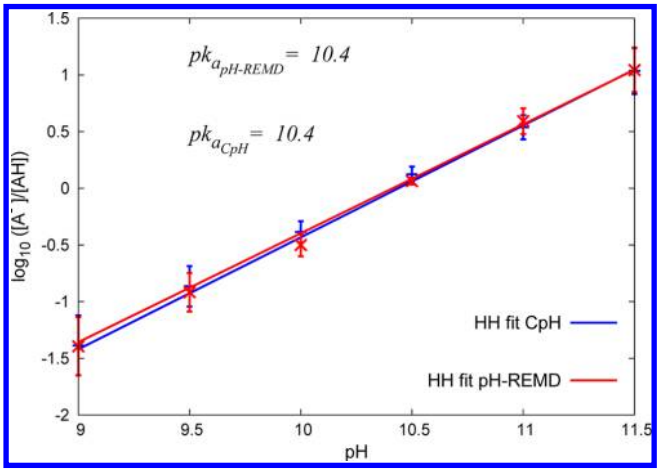

Figure 1. Comparison of Hill plots between pH-REMD and CpH methods for the Lys reference model.

4.0. Asp4 is close to the COO^- terminal, which makes its pK_a be shifted above 4.0.

The plotted titration curves of Asp2 and Asp4 in Figure 2 show that of the curves, Asp2 is shifted to the left of the model

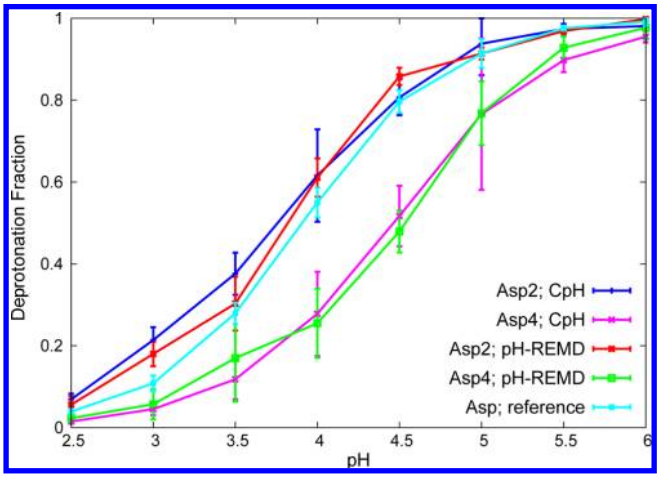

Figure 2. The titration curves of Asp side chains in ADFDA computed by both constant pH MD (blue and purple) and pH-REMD (red and green) methods. The titration curve of Asp for the reference compound (light blue) is also shown.

compound, while the curve for Asp4 is shifted to the right. There is good agreement between the pH-REMD and CpH curves. The predicted pK_as and Hill coefficients for both methods have been calculated by linear fitting on a Hill plot. Table 2 shows that the results of both methods are identical. It is worth noting that the free-energy difference associated with the two different pK_as is 0.96 kcal/mol, which highlights the sensitivity of the method to very small environmental changes.

To gauge the comparative efficiency of CpH and pH-REMD, we show, in Figure 3, that the cumulative average protonation fractions of Asp2 and Asp4 for both methods at pH = 4.0 have

dx.doi.org/10.1021/jp303385x | J. Phys. Chem. B 2012, 116, 8805−8811

Table 2. pK_a Prediction and Hill Coefficient of Fitted from the HH Equation

	ASP2		ASP4	
	pH	Hill coefficient	pH	Hill coefficient
pH-REMD	3.8 ± 0.1	0.89	4.5 ± 0.1	0.88
CpH	3.8 ± 0.1	0.91	4.5 ± 0.1	0.86

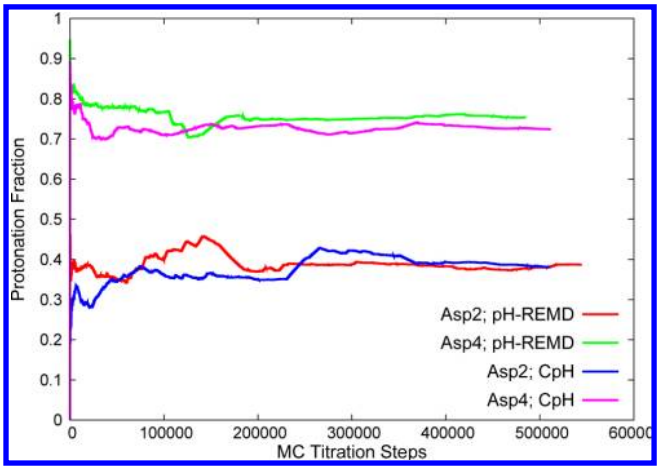

Figure 3. Cumulative average protonation fractions of Asps' side chains in ADFDA versus MC titration steps at pH = 4.0.

been plotted. The data clearly show that for both titratable groups, pH-REMD shows a faster convergence in protonation space when compared to the regular CpH method.

3. Heptapeptide Derived from OMTKY3. We applied the pH-REMD method to a capped heptapeptide derived from OMTKY3 (ACE-Ser-Asp-Asn-Lys-Thr-Tyr-Gly-NME). Dlugosz and Antosiewicz[28,29] studied this heptapeptide, and they predicted the pK_a of 4.24 for Asp3 using their CpH MD method. According to NMR experiments,[30,31] the pK_a of Asp in this heptapeptide is about 3.6. From a Hill plot, the pK_a of the three titratable groups has been calculated with the results presented in Table 3. Our computed values for the Asp3 pK_a of 3.7 (CpH) and 3.6 (pH-REMD) are in excellent agreement with the experimental value. The titration curves are shown in Figure 4.

Table 3. pK_a Values of the Titratable Residues in the Heptapeptide Derived from OMKTY3

	Asp3	Lys5	Tyr7
pH-REMD	3.6 ± 0.2	10.6 ± 0.1	10.1 ± 0.1
CpH	3.7 ± 0.2	10.6 ± 0.1	9.9 ± 0.1

There are two more titratable groups in the heptapeptide, that is, Lys5 and Tyr7, which we also titrated. Figure 5 presents the titration curves of Lys5 and Tyr7, with the computed pK_as listed in Table 3.

To compare the convergence speed between CpH and pH-REMD, we studied the cumulative average protonation/deprotonation fraction as a function of MC titration steps for all ionizable residues. Figure 6 shows the data for Tyr 7. It is evident that pH-REMD converges faster (and smoother) to the final protonation fraction.

While the convergence of the protonation equilibrium is crucial for the proper computation of a pK_a, the convergence of structural properties is also important. To consider this issue,

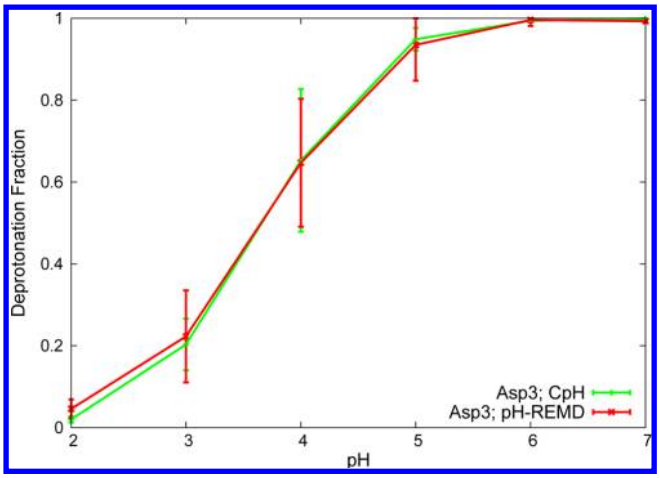

Figure 4. The titration curves of Asp3 in the heptapeptide derived from OMTKY3.

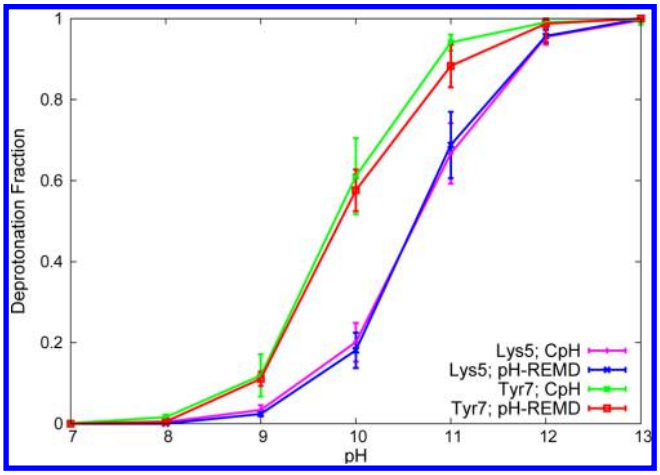

Figure 5. The titration curves of Lys5 and Tyr7 in the heptapeptide derived from OMTKY3.

we calculated the rmsd of α-carbons for all pHs (for both CpH and pH-REMD simulations) with respect to the average structure of the CpH simulation at pH 10. For both CpH and pH-REMD methods, the conformational convergence has been studied by calculation of the Kullback–Leibler divergence (see Appendix B) of rmsd cumulative distributions versus time. This is a measure of the rate of convergence to the final conformational ensemble. We presented results for both CpH and pH-REMD at pH 10 for every 100 ps (Figure 7). We used the final rsmd distribution of the CpH simulation at pH 10 as a reference for the plot. As the inset of Figure 7 shows, both simulations converge to the same rmsd distribution. It is clear that pH-REMD shows a faster and smoother conformational convergence than CpH. We also compared the rate of visiting distinct structures by calculating the rmsd autocorrelation at all pH's for both methods. According to Figure 8, the correlation times of rmsd's in pH-REMD simulations are significantly shorter than those of CpH simulations, which implies that pH-REMD visits distinct conformations more often than CpH.

■ CONCLUSIONS

In the present work, we use a combination of Hamiltonian REMD with constant pH MD to create what we call pH-REMD. The predicted pK_a for a number of systems using pH-

dx.doi.org/10.1021/jp303385x | J. Phys. Chem. B 2012, 116, 8805–8811

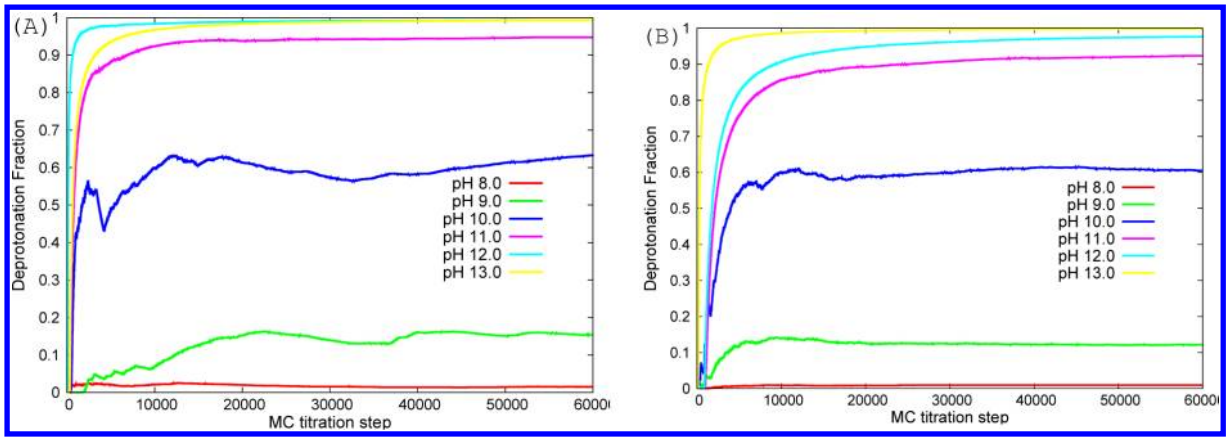

Figure 6. Cumulative average protonation fraction for TYR7 versus MC titration steps at pH = 8.0−13.0. A Comparison between the CpH (A) and the pH-REMD (B) methods.

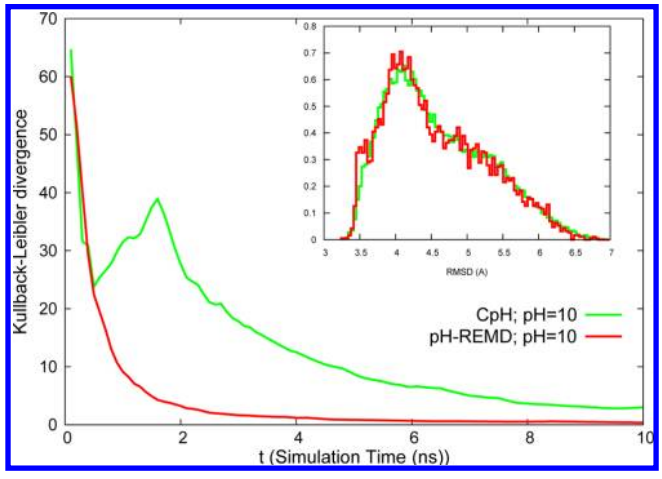

Figure 7. The Kullback−Leibler divergence measure of rmsd distributions of CpH (green) and pH-REMD (red) with respect to the final rmsd distribution in CpH. The inset shows the rmsd distributions of CpH (green) and pH-REMD (red) after 100 and 10 ns, respectively.

REMD is in excellent agreement with experimental data. Compared to CpH MD, pH-REMD converges faster in both conformational and protonation spaces. In contrast, for the temperature replica exchange molecular dynamics methods (T-REMD) in pH-REMD, the replica ladder (pH) is very limited; therefore, the overlap of energy and consequently the exchange ratio between neighboring replicas are always high. This new method is expected to perform very well for biosystems with highly coupled conformational and protonation states, like proteins with pH-dependent structure and dynamics.

APPENDIX A: PH-REMD

According to the H-REMD algorithm, each replica runs a distinct Hamiltonian. In pH-REMD, each replica runs a CpH MD simulation at a unique pH, and regularly, a swap of conformations between two adjacent replicas is attempted. Using the detailed balance condition, we can write an equilibrium proposition for the ensemble before and after an exchange is attempted.

$$P(\mathrm{X})w(\mathrm{X} \rightarrow \mathrm{X}') = P(\mathrm{X}')w(\mathrm{X}' \rightarrow \mathrm{X}) \quad \text{(A1)}$$

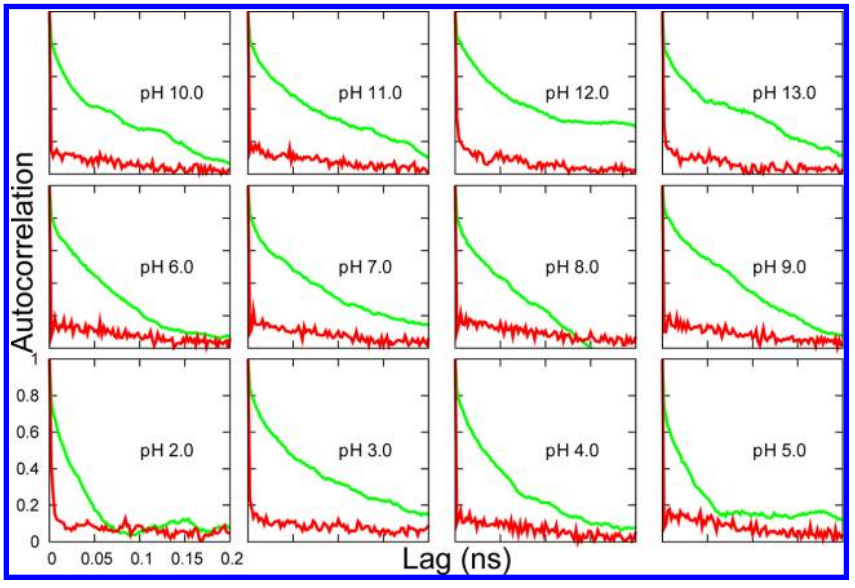

Figure 8. The rmsd autocorrelation for CpH (green) and pH-REMD (red) at all pHs.

dx.doi.org/10.1021/jp303385x | J. Phys. Chem. B 2012, 116, 8805−8811

where $P(X)$ is the probability of being at state X and $w(X \rightarrow X')$ is the probability of transition from state X to state X′.

At the exchange moment, if we only swap the conformations between two adjacent replicas and keep the protonation state unchanged, then the generalized states of X and X′ can be written as

$$X = \begin{pmatrix} q_1 & \cdots & q_i & q_j & \cdots & q_N \\ n_1 & \cdots & n_i & n_j & \cdots & n_N \end{pmatrix} \quad \text{and} \quad X' = \begin{pmatrix} q_1 & \cdots & q_j & q_i & \cdots & q_N \\ n_1 & \cdots & n_i & n_j & \cdots & n_N \end{pmatrix}$$

Here, q represents a conformation, and n represents protonation states. The ith column is related to the ith replica.

Because all N replicas are independent, the probability of the system being in the generalized state X can be written as $P(X) = \prod_{i=1}^{N} p_i(q_i,n_i)$, where $p_i(q_i,n_i)$ is the probability of replica i at conformation q_i and protonation state n_i.

Substituting those in eq A1 will result in

$$\frac{w(X \rightarrow X')}{w(X' \rightarrow X)} = \frac{p_i(q_j, n_i)p_j(q_i, n_j)}{p_i(q_i, n_i)p_j(q_j, n_j)} \tag{A2}$$

In the canonical ensemble regime (NVT) and using the Boltzmann distribution as a limiting ensemble, this can be written as

$$\frac{w(X \rightarrow X')}{w(X' \rightarrow X)} = \frac{\exp(-\beta H(q_j, n_i))\exp(-\beta H(q_i, n_j))}{\exp(-\beta H(q_i, n_i))\exp(-\beta H(q_j, n_i))} = \exp(-\Delta) \tag{A3}$$

where

$$\Delta = -\beta(H(q_i, n_i) - H(q_i, n_j) + H(q_j, n_j) - H(q_j, n_i))$$

$$\text{and} \quad \beta = 1/k_B T$$

This setup can be realized by setting the exchange probability according to the Metropolis MC criteria as

$$w(X \rightarrow X') = w((q_i, n_i); (q_j, n_j) \rightarrow (q_j, n_i); (q_i, n_j)) = \min(1, \exp(-\Delta))$$

In computing Δ, only the potential energies are required. Becuase the two exchanging replicas are running at the same temperature and have the same number and mass of particles, the kinetic energy terms will cancel each other.

APPENDIX B: KULLBACK–LEIBLER DIVERGENCE

Kullback–Leibler divergence[60,61] or relative entropy is defined as

$$D_{K-L}(X||Y) = \sum_i X(i)\log(X(i)/Y(i)) \tag{B1}$$

where X and Y are the probability distributions of a discrete random variable. It is the average, over the distribution X, of the logarithmic difference between the probabilities X and Y. It measures the degree to which X is distinguishable from Y. A small value of D indicates that X and Y are highly overlapped. This metric can be used as a measure of convergence rate, where Y is a target (or reference) distribution and X is changing by time.

AUTHOR INFORMATION

Corresponding Author

*E-mail. roitberg@ufl.edu.

Notes

The authors declare no competing financial interest.

ACKNOWLEDGMENTS

This work is supported by the National Institute of Health under Contract 1R01 AI073674. Computer resources and support were provided by the Large Allocations Resource Committee through Grant TG-MCA05S010 and the University of Florida High-Performance Computing Center.

REFERENCES

(1) Bierzynski, A.; Kim, P. S.; Baldwin, R. L. *Proc. Natl. Acad. Sci. U.S.A.* **1982**, *79*, 2470–2472.
(2) Shoemaker, K. R.; Kim, P. S.; Brems, D. N.; Marqusee, S.; York, E. J.; Chaiken, I. M.; Stewart, J. M.; Baldwin, R. L. *Proc. Natl. Acad. Sci. U.S.A.* **1985**, *82*, 2349–2353.
(3) Schaefer, M.; Van Vlijmen, H. W. T.; Karplus, M. *Adv. Protein Chem.* **1998**, *51*, 1–57.
(4) Demchuk, E.; Genick, U. K.; Woo, T. T.; Getzoff, E. D.; Bashford, D. *Biochemistry* **2000**, *39*, 1100–1113.
(5) Dillet, V.; Dyson, H. J.; Bashford, D. *Biochemistry* **1998**, *37*, 10298–10306.
(6) Harris, T. K.; Turner, G. J. *IUBMB Life* **2002**, *53*, 85–98.
(7) Antosiewicz, J.; Briggs, J. M.; McCammon, J. A. *Eur. Biophys. J.* **1996**, *24*, 137–141.
(8) Hunenberger, P. H.; Helms, V.; Narayana, N.; Taylor, S. S.; McCammon, J. A. *Biochemistry* **1999**, *38*, 2358–2366.
(9) Hill, T. L. *J. Am. Chem. Soc.* **1956**, *78*, 1577–1580.
(10) Simonson, T.; Carlsson, J.; Case, D. A. *J. Am. Chem. Soc.* **2004**, *126*, 4167–4180.
(11) Tanford, C.; Kirkwood, J. G. *J. Am. Chem. Soc.* **1957**, *79*, 5333–5339.
(12) Warshel, A. *Nature* **1987**, *330*, 15–16.
(13) Mongan, J.; Case, D. A.; McCammon, J. A. *J. Comput. Chem.* **2004**, *25*, 2038–2048.
(14) Baptista, A. M.; Martel, P. J.; Petersen, S. B. *Proteins* **1997**, *27*, 523–544.
(15) Borjesson, U.; Hunenberger, P. H. *J. Chem. Phys.* **2001**, *114*, 9706.
(16) Khandogin, J.; Brooks, C. L. *Biophys. J.* **2005**, *89*, 141–157.
(17) Khandogin, J.; Brooks, C. L. *Biochemistry* **2006**, *45*, 9363–9373.
(18) Khandogin, J.; Brooks, C. L. *Proc. Natl. Acad. Sci. U.S.A.* **2007**, *104*, 16880–16885.
(19) Khandogin, J.; Chen, J. H.; Brooks, C. L. *Proc. Natl. Acad. Sci. U.S.A.* **2006**, *103*, 18546–18550.
(20) Khandogin, J.; Raleigh, D. P.; Brooks, C. L. *J. Am. Chem. Soc.* **2007**, *129*, 3056–3057.
(21) Mertz, J. E.; Pettitt, B. M. *Int. J. Supercomput. Ap.* **1994**, *8*, 47–53.
(22) Borjesson, U.; Hunenberger, P. H. *J. Phys. Chem. B* **2004**, *108*, 13551–13559.
(23) Baptista, A. M.; Teixeira, V. H.; Soares, C. M. *J. Chem. Phys.* **2002**, *117*, 4184.
(24) Machuqueiro, M.; Baptista, A. M. *Biophys. J.* **2006**, *92*, 1836–1845.
(25) Machuqueiro, M.; Baptista, A. M. *Proteins: Struct., Funct., Bioinf.* **2008**, *72*, 289.
(26) Machuqueiro, M.; Baptista, A. M. *J. Am. Chem. Soc.* **2009**, *131*, 12586–12594.
(27) Burgi, R.; Kollman, P. A.; van Gunsteren, W. F. *Proteins* **2002**, *47*, 469–480.
(28) Dlugosz, M.; Antosiewicz, J. M. *Chem. Phys.* **2004**, *302*, 161–170.

(29) Dlugosz, M.; Antosiewicz, J. M. *J. Phys. Chem. B* **2005**, *109*, 13777−13784.
(30) Dlugosz, M.; Antosiewicz, J. M. *J. Phys.: Condens. Matter* **2005**, *17*, S1607.
(31) Dlugosz, M.; Antosiewicz, J. M.; Robertson, A. D. *Phys. Rev. E* **2004**, *69*, 021915−021924.
(32) Walczak, A. M.; Antosiewicz, J. M. *Phys. Rev. E* **2002**, *66*, 051911−051918.
(33) Lee, M. S.; Salsbury, F. R.; Brooks, C. L. *Proteins: Struct., Funct., Bioinf.* **2004**, *56*, 738−752.
(34) Metropolis, N.; Rosenbluth, A. W.; Rosenbluth, M. N.; Teller, A. H.; Teller, E. *J. Chem. Phys.* **1953**, *21*, 1087.
(35) Baptista, A. M. *J. Chem. Phys.* **2002**, *116*, 7766−7768.
(36) Machuqueiro, M.; Baptista, A. M. *J. Phys. Chem. B* **2006**, *110*, 2927−2933.
(37) Case, D. A.; Darden, T. A.; Cheatham, I.; Simmerling, C. L.; Wang, J.; Duke, R. E.; Luo, R.; Crowley, M.; Walker, R. C.; Zhang, W. et al. *AMBER 10*; University of California: San Francisco, CA, 2008.
(38) *Methods in Enzimology*; Johnson, M. L., Brand, L., Eds.; Academic Press: San Diego, Burlington, London, 2009; Vol. *467*.
(39) Warwicker, J. *Protein Sci.* **2004**, *13*, 2793−2805.
(40) Barth, P.; Alber, T.; Harbury, P. B. *Proc. Natl. Acad. Sci. U.S.A.* **2007**, *104*, 4898−4903.
(41) Li, H. Z.; Fajer, M.; Yang, W. *J. Chem. Phys.* **2007**, *126*, 024106.
(42) Mitsutake, A.; Sugita, Y.; Okamoto, Y. *Biopolymers* **2001**, *60*, 96−123.
(43) Zheng, L. Q.; Chen, M. G.; Yang, W. *J. Chem. Phys.* **2009**, *130*, 234105.
(44) Sugita, Y.; Okamoto, Y. *Chem. Phys. Lett.* **1999**, *314*, 141−145.
(45) Lyubartsev, A. P.; Martsinovski, A. A.; Shevkunov, S. V.; Vorontsov-Velyaminov, P. N. *J. Chem. Phys.* **1992**, *96*, 1776.
(46) Berg, B. A.; Neuhaus, T. *Phys. Lett. B* **1991**, *267*, 249−253.
(47) Berg, B. A.; Neuhaus, T. *Phys. Rev. Lett.* **1992**, *68*, 9−12.
(48) Laio, A.; Parrinello, M. *Proc. Natl. Acad. Sci. U.S.A.* **2002**, *99*, 12562−12566.
(49) Itoh, S. G.; Damjanović, A.; Brooks, B. R. *Proteins: Struct., Funct., Bioinf.* **2011**, *79*, 3420−3436.
(50) Wallace, J. A.; Shen, J. K. *J. Chem. Theory Comput.* **2011**, *7*, 2617−2629.
(51) Wallace, J. A.; Wang, Y.; Shi, C.; Pastoor, K. J.; Nguyen, B.; Xia, K.; Shen, J. K. *Proteins: Struct., Funct., Bioinf.* **2011**, *79*, 3364−3373.
(52) Meng, Y.; Roitberg, A. E. *J. Chem. Theory Comput.* **2010**, *6*, 1401−1412.
(53) Meng, Y.; Sabri Dashti, D.; Roitberg, A. *J. Chem. Theory Comput.* **2011**, *7*, 2721−2727.
(54) Mongan, J.; Case, D. A. *Curr. Opin. Struct. Biol.* **2005**, *15*, 157−163.
(55) Williams, D. H.; Stephens, E.; O'Brien, D. P.; Zhou, M. *Angew. Chem., Int. Ed.* **2004**, *43*, 6596−616.
(56) Hornak, V.; Abel, R.; Okur, A.; Strockbine, B.; Roitberg, A.; Simmerling, C. *Proteins: Struct., Funct., Bioinf.* **2006**, *65*, 712−725.
(57) Ryckaert, J. P.; Ciccotti, G.; Berendsen, H. J. C. *J. Comput. Phys.* **1977**, *23*, 327−341.
(58) Onufriev, A.; Bashford, D.; Case, D. A. *J. Phys. Chem. B* **2000**, *104*, 3712−3720.
(59) Sindhikara, D.; Meng, Y.; Roitberg, A. E. *J. Chem. Phys.* **2008**, *128*, 024103.
(60) McClendon, C. L.; Hua, L.; Barreiro, G.; Jacobson, M. P. *J. Chem. Theory Comput.* **2012**, *8*, 2115−2126.
(61) Hamacher, K. *J. Comput. Chem.* **2007**, *28*, 2576−2580.